11th Canadian Masonry Symposium, Toronto, Ontario, May 31- June 3, 2009

INFLUENCE OF VERTICAL REINFORCEMENT AND LATERAL CONFINEMENT ON THE AXIAL CAPACITY OF MASONRY WALLS

A. Paturova[1], B.F. Sparling[2] and L.D. Wegner[3]

[1] Structural Engineer, AMEC Americas Ltd., #301 - 121 Research Drive, Saskatoon, SK, S7N 4L8, anna.paturova@amec.com

[2] Professor, Department of Civil and Geological Engineering, University of Saskatchewan, Saskatoon, SK, S7N 5A9, Canada, bruce.sparling@usask.ca

[3] Associate Professor, Department of Civil and Geological Engineering, University of Saskatchewan, Saskatoon, SK, S7N 5A9, Canada, leon.wegner@usask.ca

ABSTRACT

An experimental study was undertaken to investigate the influence of vertical reinforcement and lateral confinement on the axial strength and ductility of short, partially grouted concrete masonry block walls. Three types of test specimens were considered: unreinforced specimens with a grouted cell; specimens with a grouted cell and vertical reinforcement; and specimens with a grouted cell, vertical reinforcement and lateral confinement placed within the grouted cell. A total of thirty wall specimens, each 1000 mm high by 590 mm wide, were constructed in running bond using standard 200 mm hollow concrete masonry blocks; the central cell of each specimen was grouted. The wall specimens were tested monotonically to failure under axial loading. In addition to the applied load, axial displacements were measured at 14 locations to determine both overall axial deformations and average strains. Cracking patterns and failure modes were also monitored and recorded. Test results indicated that vertical reinforcement in the grouted cores did not have a significant effect on the axial strength of the wall specimens. Due to problems with ensuring adequate compaction of the grout, lateral confinement provided by spiral reinforcement within the cells actually caused a slight reduction in the average axial strength. On the other hand, both the vertical reinforcement and lateral confinement tended to increase the post-peak ductility of the walls. The dominant failure mode observed in all three types of wall specimens featured vertical cracking that progressed through the end webs of the specimens, followed by compressive spalling in the face shell.

KEYWORDS: concrete masonry walls, axial strength, reinforcement, confinement, ductility

INTRODUCTION

In conventional practice, full or partial grouting is the primary method used to increase the compressive capacity of walls constructed with hollow concrete masonry blocks. Vertical reinforcement, when present, is used to augment the flexural strength of the wall, but is generally neglected in the calculation of axial strength.

The role of lateral confinement in enhancing the effectiveness of longitudinal reinforcement in reinforced concrete has long been established [1]. In particular, spiral reinforcement is known to increase both the strength and ductility of reinforced concrete columns by inducing a state of tri-axial compression into the concrete core and compensating for the loss of the outer concrete shell due to compressive spalling [2].

The influence of lateral confinement in reinforced masonry walls, though, has not been investigated as thoroughly. It is generally conceded that vertical reinforcement, by itself, does not significantly affect the axial strength of grouted concrete masonry walls [3, 4]. There is some evidence, however, that the presence of lateral confinement, either in the form of steel plates inserted into the mortar beds [4] or wire mesh placed in the grouted cells [5], has a beneficial effect on both the axial strength and overall ductility of grouted concrete masonry.

In the current study, the influence of vertical reinforcement and lateral confinement on the compressive behaviour of short, partially grouted concrete masonry walls is investigated further. Specifically, lateral confinement provided by spirals placed within the grouted cells of hollow concrete masonry blocks is considered.

DESCRIPTION OF EXPERIMENTAL PROGRAM

A total of 30 concrete block masonry wall specimens were tested to failure under monotonically increasing concentric axial loading. The specimens were constructed on site by a qualified mason in the Structural Laboratory at the University of Saskatchewan.

As shown in Figure 1, each wall specimen was 590 mm wide by five courses high and built in running bond using standard 200 mm concrete masonry blocks with a nominal compressive strength of 15 MPa. Type S mortar conforming to the requirements of CSA Standard S304.1-04 [6] was used throughout. Standard No. 8 ASWG (4.1 mm diameter) ladder-type joint reinforcement was placed in every bed joint. One week following the construction of the wall, the central cell in each wall specimen was grouted using a fine grout having a minimum slump of 250 mm that was provided by a local concrete supplier; the grout was carefully consolidated using an electric needle vibrator until the first sign of bleeding was observed.

As illustrated in Figure 2, three types of wall specimens were investigated, differing only in the reinforcing details within the central cell. Ten specimens of each type were tested. Type A specimens featured a grouted central cell with no vertical or lateral reinforcement. The grouted central cells in Type B specimens were reinforced with a single No. 15 Grade 400 vertical reinforcing bar. To ensure that the vertical reinforcement was fully effective in the upper portions of the wall specimens, a bearing plate was welded to the top end of the vertical rebar (see Figure 2b), sized to produce yielding in the reinforcement at applied loads near the anticipated failure condition. Similarly, a No. 15 dowel anchored in the concrete base was used to maintain the full effectiveness of the vertical reinforcement in the lower portions of the wall. Type C specimens were similar to those of Type B, with the exception that spiral lateral reinforcement was added to the grouted cells. The spiral reinforcement was fabricated using No. 6 ASWG (4.88 mm diameter) wire made from 1080 steel with a nominal yield strength of 400 MPa; the spirals featured an outside diameter of 110 mm and a pitch of 15 mm.

After proper curing, the specimens were carefully lifted onto the testing machine using lift hooks anchored into the concrete bases of the specimens (see Figure 1).

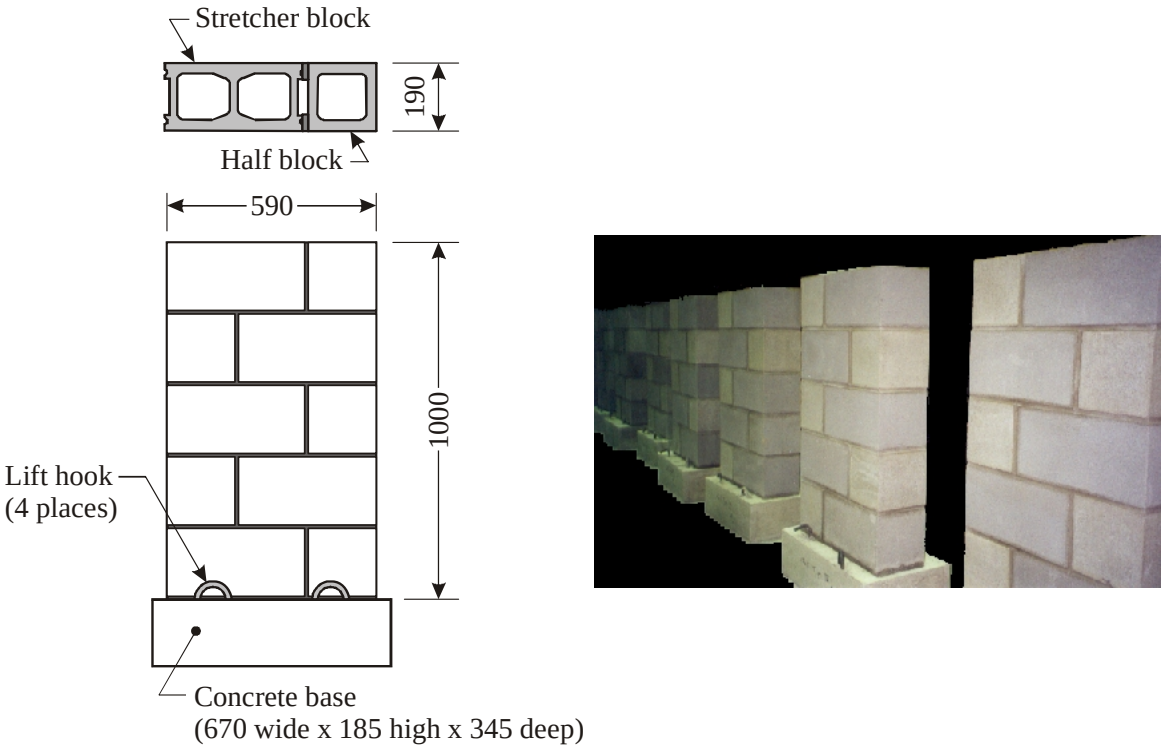

Figure 1: Description of wall specimens.

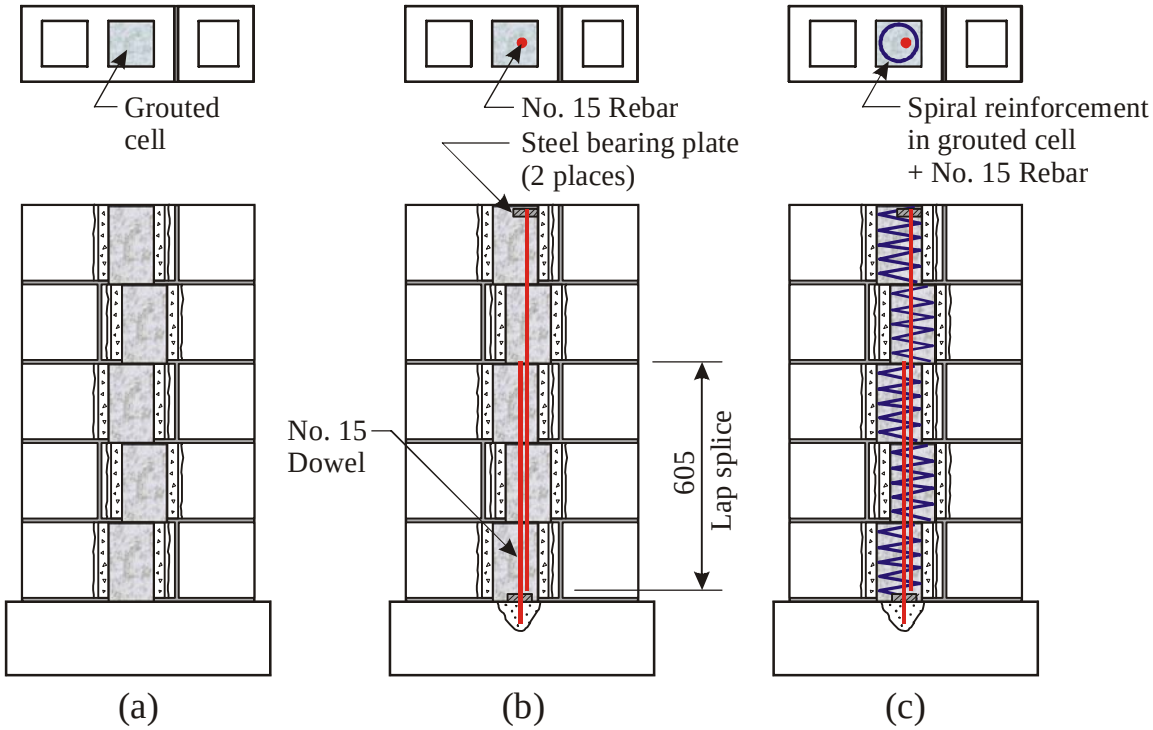

Figure 2: Cutaway section showing central cell reinforcing details: (a) Type A wall specimen; (b) Type B wall specimen; and (c) Type C wall specimen.

The test set-up is shown schematically in Figure 3. To promote uniform loading across the width of the specimens, a steel spreader beam and 10 mm fibre board layer were positioned between the loading head of the test machine and top of the wall specimen. Instrumentation consisted of one load cell (Model 1100/200-K, Artech Industries, CA) placed directly below the loading head and 14 linear displacement transducers (Models HS10 and HS50, Measurement Group Inc., Rayleigh, NC) placed as shown on Figure 3 and calibrated to read increments of ±0.0001 mm. Readings from the load cell and displacement transducers were recorded electronically at two second intervals during the testing period using a National Instruments™ data acquisition system controlled by LabVIEW™ software. A horizontal steel arm was attached at mid-width of the second and fourth courses on the front face of the specimens, as well as directly below the spreader beam, to permit the mounting of displacement transducers used to monitor both axial displacements and flexural deformations taking place about the strong axis of the wall.

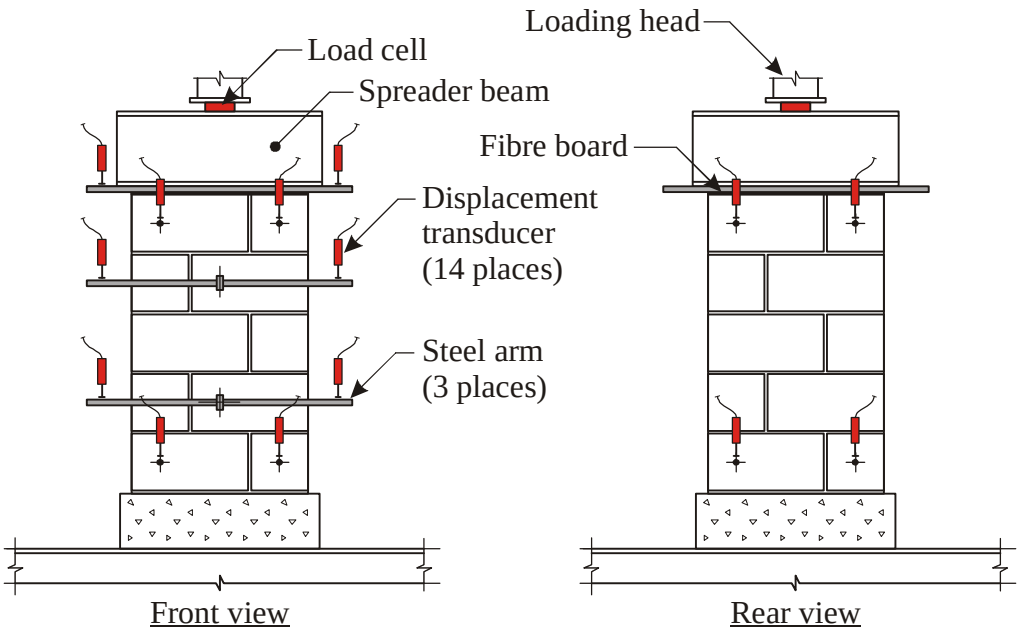

Figure 3: Wall specimen test set-up and instrumentation layout.

Quasi-static axial load was applied monotonically to failure at a rate of approximately 5 kN per minute. Load and deflection readings were obtained over the entire testing period, including in the post-peak region; to prevent damage to the sensors, though, displacement transducers mounted directly on the specimen were removed prior to failure. During the loading process, cracking loads were noted and crack progressions photographed. After removing the failed specimen from the testing machine, the central grouted cell was uncovered and photographed.

Additional material testing was also carried out on masonry components and assemblages. Ten 75 x 150 mm mortar cylinders were cast and tested, yielding an average compressive strength of 12.4 MPa and an average modulus of elasticity of 8.8 GPa. For the grout, test specimens using both non-absorbent and absorbent moulds were considered. First, ten 75 x 150 mm grout cylinders were cast in non-absorbent moulds, yielding an average compressive strength of 17.1 MPa and an average elastic modulus of 21.1 GPa. Next, ten 100 x 100 x 190 mm grout prisms were cast using paper-lined standard concrete masonry blocks as absorbent forms; the

average compressive strength from the grout prisms was found to be 20.6 MPa. Finally, ten ungrouted masonry prisms, each three courses high, were constructed in stack bond using standard 200 mm stretcher blocks. The average compressive strength of the masonry prisms was found to be 10.3 MPa, based on the estimated effective mortar bed area.

EXPERIMENTAL RESULTS

Comparisons of the failure loads attained by the different wall specimen types are provided in Table 1 and Figure 4. In this context, the failure load is defined as the peak applied axial load supported by the specimen prior to failure. Included in these results are the maximum, minimum and mean failure loads for the ten specimens constructed with each of the three reinforcement configurations shown in Figure 2. Table 1 also provides the corresponding mean ultimate strength of the three specimen types, defined as the mean failure load divided by a nominal effective area of the mortar bed joint and grout (taken to be 67.0×10^3 mm^2), as well as the coefficient of variation of the recorded failure loads.

Table 1: Wall specimen failure load statistics.

Specimen Type	Failure Load (kN)			Ultimate Strength* (MPa)	Coefficient of Variation (%)
	Maximum	Minimum	Mean		
Type "A"	935	647	801	11.9	12.5
Type "B"	950	650	793	11.8	12.2
Type "C"	1031	538	726	10.8	19.1

* Ultimate strength = Mean failure load / Nominal effective area $\left(67.0\times10^3 \text{ mm}^2\right)$

In conventional design practice, the failure of a masonry element loaded in uniform compression is assumed to be initiated when the masonry reaches a compressive strain of approximately 0.003 [6]. At that stage, fully bonded and developed vertical reinforcement in the grouted cells would

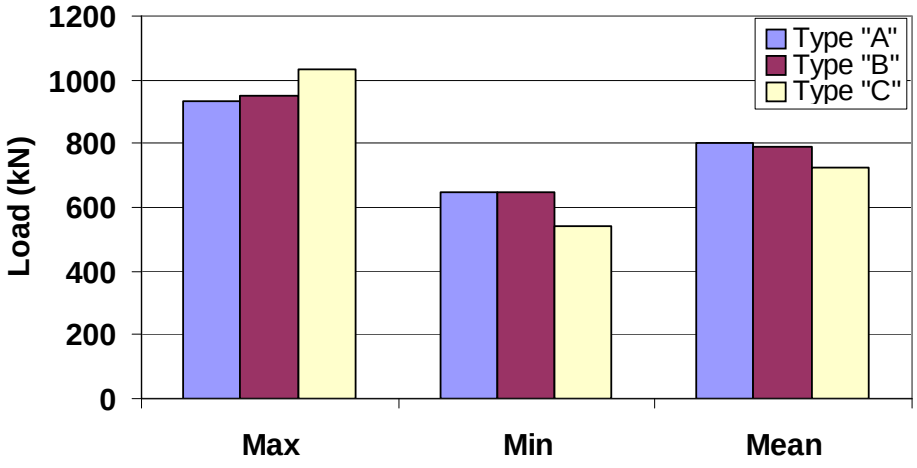

Figure 4: Failure loads for wall specimens.

have yielded completely. For the No. 15 rebar used in Types B and C specimens, the resulting compressive force in the steel (approximately 80 kN) should then have increased the compressive capacity of the wall specimens by roughly 10%, assuming that compression alone governed failure and that the reinforcing was fully effective.

Somewhat surprisingly then, the unreinforced (Type "A") specimens exhibited the highest mean failure load of 801 kN, corresponding to an ultimate strength of 11.9 MPa. Type B specimens, with vertical reinforcement, were found to have essentially the same capacity as the unreinforced walls at 793 kN, while Type C specimens, with both vertical and lateral reinforcement, yielded the lowest mean strength at 726 kN. Although the difference in mean failure loads between specimen Types A and C appeared to be notable (9.4%), it was not statistically significant at the 90% level of confidence due to the relatively high variability observed in the Type C specimen test results. Nevertheless, it appears that vertical reinforcement did not contribute in any measurable way to the compressive axial capacity of the masonry wall specimens.

The observed ineffectiveness of vertical reinforcement under axial compression may be attributed, in part, to the failure mechanism observed in the wall specimens, which differed significantly from the theoretical uniform crushing model. In every case, signs of visible distress were first detected in the form of vertical cracks appearing in the webs of the end blocks at approximately 55% to 64% of the failure load (see Figure 5a). As the load was increased further, the splitting cracks widened and extended vertically into other courses. At approximately 85% to 95% of the failure load, local crushing in the face shell adjacent to one or more of the mortar beds was observed, leading almost immediately to localized spalling of the face shell and mortar, and ultimately to what could be characterized as a tensile-compressive failure (see Figure 5b); similar failure patterns have been reported previously by others [4, 7, 8]. This failure mode may have been accentuated by the configuration of the test specimens, in which the cells at both ends of the narrow wall specimens were ungrouted and unrestrained in the lateral direction by adjacent masonry units. In a wider section of wall, ungrouted cells would generally be restrained to some degree by adjacent blocks, as well as by the continuous joint reinforcement.

The tendency for lateral expansion of the wall specimens under axial loading was also evident in the deformations experienced by the joint reinforcement, an example of which is shown in Figure 6. While not conclusive, this finding suggests that increased lateral confinement from stiffer joint reinforcement, or perhaps some other means, may be effective in delaying the formation of splitting cracks in the end faces. The use of a stainless steel plate inserted into the mortar bed has been suggested for this purpose [3].

Type C specimens, featuring both vertical reinforcement and spirals within the grouted cells, exhibited the widest range of behaviour, yielding both the highest failure load (1,031 kN) and the lowest (538 kN). An examination of the failed specimens indicated that instances of lower than expected failure loads corresponded to walls with incomplete consolidation of the grout in the lower courses (see Figure 7a), despite the care taken to vibrate the grout thoroughly during placement. It was concluded that the presence of spiral reinforcement, coupled with the inherent vertical misalignment of grouted cells in running bond construction (see Figure 7b) made it difficult to ensure proper consolidation.

(a) **(b)**

Figure 5: Typical wall crack patterns: (a) Initial cracking in end web; and (b) Tensile-compressive cracking and spalling at ultimate conditions.

Representative axial stress-strain curves for the three specimen types are shown in Figure 8. For this purpose, the axial strain averaged over the height of the wall was derived by dividing the difference between the vertical displacement readings taken at mid height of the top and bottom courses by the vertical distance between the top and bottom displacement transducers (see the displacement transducer layout in Figure 3); the axial stress was defined as the applied load divided by the effective masonry area, as described previously. It is apparent that the stress-strain behaviour was quite similar for specimens Types A and B, while the Type C specimen exhibited a relatively softer response for strains exceeding 0.001; as alluded to previously, this softer behaviour of Type C specimens was likely related to incomplete consolidation of the grout in the lower courses. All specimens were seen to feature a fairly linear stress-strain relationship at loads below approximately 60% of the failure load. Interestingly, some specimens, such as the Type A specimen depicted in Figure 8, exhibited an apparent hardening behaviour, becoming stiffer as the strain levels increased toward the ultimate condition.

Figure 6: Observed deformation of the joint reinforcement.

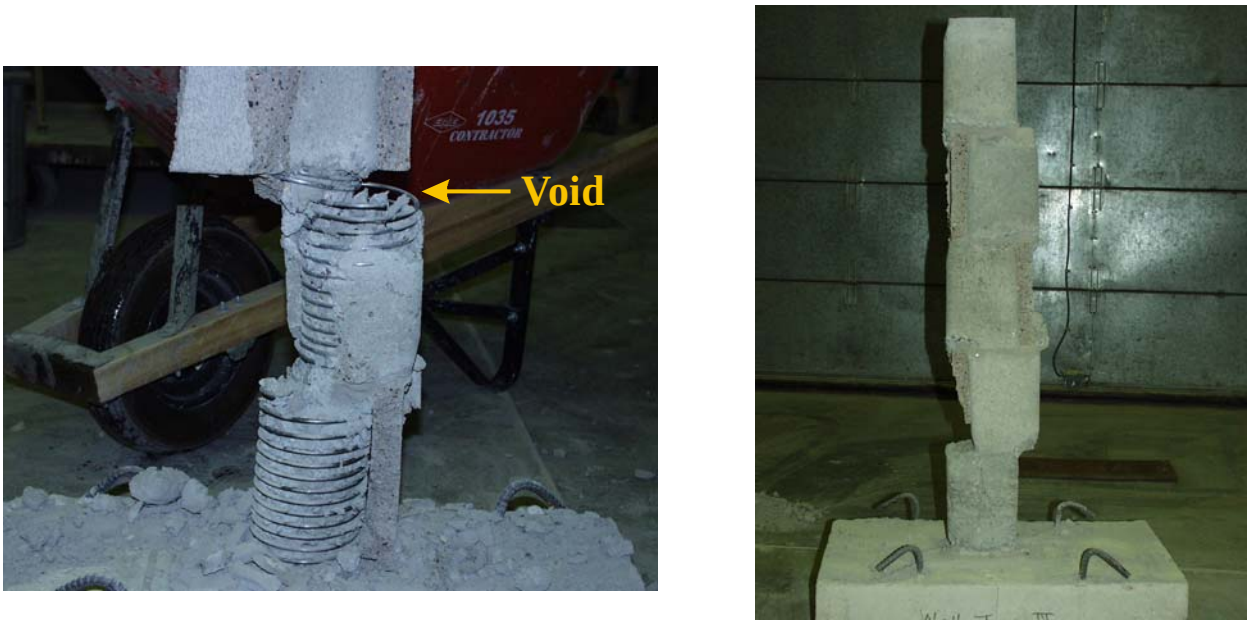

(a) **(b)**

Figure 7: Grouted columns extracted from failed wall specimens: (a) Type C specimen showing voids in grout; and (b) Type A specimen showing misalignment of cells.

Figure 9 shows representative axial load versus displacement plots that extend well beyond the ultimate load and into the post-peak region. To avoid damaging the more vulnerable instrumentation, these displacement measurements were obtained from the transducers

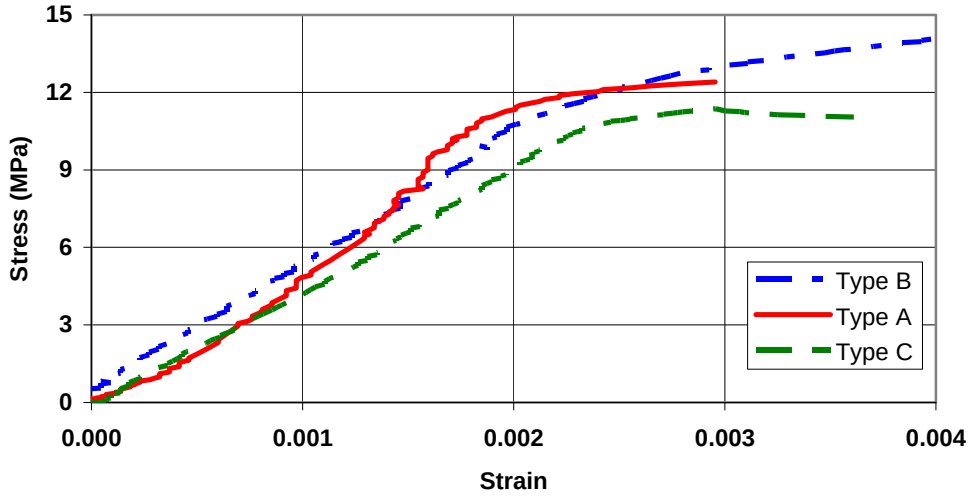

Figure 8: Representative axial stress-strain curves for each wall type, based on measured face shell displacements.

positioned at the top of the specimens (see Figure 3); as such, the displacements featured in Figure 9 include deformations of the fibre board beneath the spreader beam in addition to those of the wall specimen. Once again, the response of Types A and B specimens is nearly coincident prior to the ultimate load and very similar in the post-peak region. The Type C specimen, on the other hand, is seen to be more rigid in this case, particularly prior to ultimate conditions.

Under the displacement-controlled loading used in this study, specimens of all three types were seen to sustain substantial post-peak deformations prior to total collapse. To compare this post-peak deformation in a more quantitative manner, the average post-peak ductility was estimated for each specimen type; here, the post-peak ductility is defined as the ratio between the post-peak displacement and the displacement at ultimate conditions. The average ductility for the concrete masonry walls was found to be 39.7% for Type A specimens, 42.9% for Type B specimens and 63.0% for Type C specimens. In general, therefore, specimens with lateral confinement provided by the spirals exhibited a significantly higher degree of post-peak ductility.

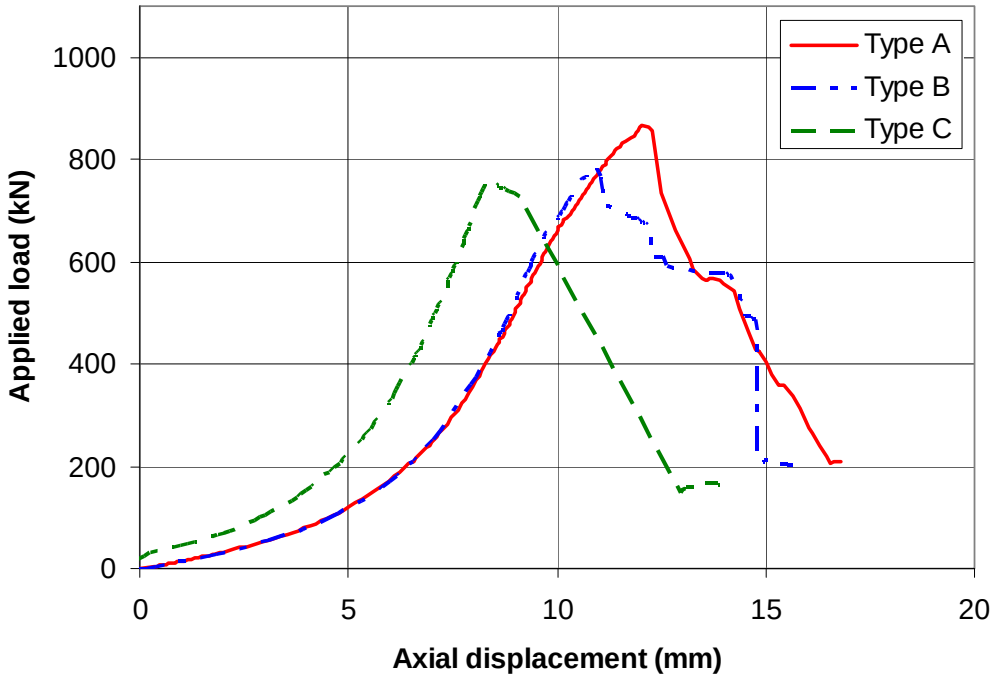

Figure 9: Representative axial load-displacement curves for each wall type, based on displacements measured at the top of the wall (including fibre board deformations).

SUMMARY AND CONCLUSIONS

An experimental study was undertaken to investigate the influence of vertical reinforcement and lateral confinement on the axial strength of partially grouted concrete masonry block walls. A total of 30 short wall specimens were constructed with three different configurations: Type A specimens featured a grouted central cell, but no reinforcement; Type B specimens contained vertical reinforcing within the grouted cells; and Type C specimens contained both vertical

reinforcement and spiral lateral confinement within the grouted cells. All the specimens were tested to failure under monotonically increasing concentric axial loading.

Test results indicated that the presence of vertical reinforcement had a negligible effect on the axial capacity of the wall specimens. Furthermore, the spiral confinement placed within the grouted cells were actually found to have a detrimental influence, on average, due to the difficulty encountered in ensuring adequate consolidation of the grout in the lowest one or two courses of the wall. All specimens failed in a tensile-compressive failure mode in which vertical cracking in the end webs of the concrete blocks was followed by crushing and spalling in the block face shells.

Displacement measurements suggested that the spiral cell reinforcement may have had a slight beneficial influence on the post-peak ductility of the specimens, compared to that of the unreinforced specimens. There was also some indication that the grout confinement provided by the spirals did stiffen the axial response in well consolidated specimens.

ACKNOWLEDGEMENTS

Financial and in-kind support from the Canadian Masonry Research Institute and the Saskatchewan Masonry Institute, along with financial support from the Natural Sciences and Engineering Research Council, are gratefully acknowledged.

REFERENCES

1. Moehle, J.P. and Cavanagh T. (1985) “Confinement Effectiveness of Crossties in RC”. Journal of Structural Engineering, Vol. 111, No. 10, pp. 2105-2119.
2. Pessiki, S. and Pieroni, A. (1997) “Axial load behavior of large-scale spirally-reinforced high-strength concrete columns”. ACI Structural Journal, Vol. 94, No. 3, pp. 304-314.
3. Priestley, M.J.N. and Elder, D.M. (1983) “Stress-Strain Curves for Unconfined and Confined Concrete Masonry”. ACI Journal, Vol. 80, No. 3, pp. 192-201.
4. G.C. Hart, N. Sajjad, G.R. Kingsley and J.L. Noland. (1989) “Analytical Stress-Strain Curves for Grouted Concrete Masonry”. TMS Journal, Vo1. 8, No. 1, pg. 21-34.
5. Dhanasekar, M. and Shrive, N.G. (2002) “Strength and Deformation of Confined and Unconfined Grouted Concrete Masonry”, ACI Structural Journal, Vol. 99, No. 6, pp. 819-826.
6. CSA (2004) Design of Masonry Structures. CSA Standard S304.1-04, Canadian Standards Association, Mississauga, ON, Canada.
7. Hamid, A.A. and Drysdale, R.G. (1979) “Suggested Failure Criteria for Grouted Concrete Masonry under Axial Compression”. ACI Journal, Vol. 76, No. 10, pp. 1047-1061.
8. Hamid, A.A. and Chandrakeerthy, S.R. (1992) “Compressive Strength of Partially Grouted Concrete Masonry Using Small Scale Wall Elements”. TMS Journal, Vol. 11, No. 1, pp. 75-85.